



Flow rate calculations based on rheometric measurements of model waxy oils at different surface roughness

Thiago O. Marinho¹ · Márcia C. K. de Oliveira² · Antônio M. C. Maciel² · André S. Guimarães¹ · Márcio Nele¹

Received: 31 October 2022 / Revised: 2 September 2023 / Accepted: 17 September 2023 / Published online: 16 October 2023
© The Author(s) under exclusive licence to Associação Brasileira de Engenharia Química 2023

Abstract

Waxy gels can be formed during offshore production upon cooling waxy crude oils at sufficiently low temperatures. This fact is relevant to the petroleum industry, as severe issues can arise during crude oil production, storage, and transportation when precipitation and aggregation of paraffin wax crystals occur. In this study, the slippage effects during rheometric measurements were quantified, and its impact on flow rate calculations and restart pressure drop were evaluated. Model waxy gels consisting of a macrocrystalline wax added to mineral oil (3.0 and 7.5 wt%) were employed. The gels were formed in situ in a stress-controlled rheometer, and rheological properties were obtained by dynamic oscillatory and steady-state experiments. Different geometry configurations, including smooth and grooved concentric cylinders, were tested. Flow curves were adjusted by Power Law and Herschel–Bulkley models, and the parameters were used in modified Poiseuille equations to estimate the flow rate for specific pressure drop and clogged pipeline length. The rheological data obtained with smooth surfaces were significantly affected by the slippage effects (e.g., yield stress ~80% smaller), which was reflected by exceedingly high flow rates, especially for the Power Law model. The Herschel–Bulkley model provided more realistic estimates, i.e., with flow rate tending to zero for a sufficient long pipeline, given realistic yield stresses. Since it is very difficult to predict the failure mechanism of a gelled waxy oil in a real production scenario (i.e., adhesive or cohesive failure), this work can provide helpful information for designing pipelines and transportation systems.

Keywords Yield stress · Apparent wall slip · Flow assurance · Flow rate · Restart production

Introduction

Waxy gels can be formed under appropriate thermodynamic conditions at offshore petroleum production. The crystal precipitation initiates at the Wax Appearance Temperature (WAT) upon the cooling of waxy crude oils due to the heat loss to the cold seabed environment (~4 °C). Moreover, a subsequent wax deposition can reduce the flow area, resulting in partial pipeline blockage, despite precipitation and

deposition occurring during crude oil production. Although, the situation can be aggravated if the operations are interrupted during emergencies or maintenance. In this scenario, the petroleum located inside the pipeline can undergo a gelation process, and the pipeline can become clogged with waxy gel (Petter Rønningsen 1992; Chang et al. 1998; Davidson et al. 2004; Aiyejina et al. 2011; Cabanillas et al. 2016). Thus, the proper design of transport processes involving waxy crude oils should account for this possibility.

The gels' rheological behavior can be complex since elasto-viscoplastic, thixotropic, and yield-stress characteristics are present (Chang et al. 1998; Visintin et al. 2005). One big challenge in correctly characterizing waxy gels' rheology is the presence of apparent wall slip phenomenon during rheometric tests. This can lead to underestimated yield stress (σ_y) and viscosity values and affect data reproducibility (Barnes 1995; Walls et al. 2003). Therefore, the subsequent steps for the pipeline design can be influenced by this experimental artifact to a great extent because (i) underestimated yield stress may lead to projects with

This is an invited, extended version of the manuscript presented in the 1st Flow Assurance Technology Congress and published in the FATC22 Anais.

✉ Thiago O. Marinho
tmarinho@peq.coppe.ufrj.br

¹ PEQ/COPPE, Federal University of Rio de Janeiro, Rio de Janeiro 21941-909, Brazil

² Petrobras/CENPES, University City, Rio de Janeiro 21941-909, Brazil

insufficient pump capacity, as it effectively determines the pressure required to initiate or restart the pipeline flow (Davidson et al. 2004) and (ii) underestimated viscosity may lead to exceeding high productivity estimates.

Apparent wall slip emerges in the context of different flow heterogeneities that yield stress materials might exhibit. The conditions that favor this phenomenon are encountered when low shear rates, large components in the disperse phase, smooth walls, and small dimensions are present (Barnes 1995; Cloitre and Bonnecaze 2017). Therefore, waxy oils, tested at the rheometer with smooth geometries, are prone to present slippage effects under cooling conditions.

In the case of colloidal systems such as waxy gels, apparent wall slip is likely caused by the development of a macroscopic solvent-rich layer at the sample-wall interface, also termed the "depleted layer" (Saak et al. 2001). Figure 1 presents schematics of velocity profiles in simple shear for homogeneous flow, shear-banded flow, true slip flow, and apparent slip flow. In the first case, the velocity profile varies linearly between the shearing surfaces, and the resulting local shear rates are equal to the macroscopic shear rates (Fig. 1A). Shear banding denotes a broad class of phenomena of different origins (e.g., material instabilities), which are associated with the spatial localization of the strain or shear rate into one or several layers of a finite thickness (Fig. 1B) (Hatzikiriakos 2015). Slip, in turn, represents an extreme realization of strain localization, where most of the deformation occurs near the confining walls, whereas the material bulk behaves like a rigid body with negligible deformation. It is essential to distinguish the true slip phenomenon, where the slip layer has a molecular dimension (Fig. 1C), from apparent wall slip, where the local velocity varies over a finite, albeit small, mesoscopic distance (Fig. 1D). True slip is relevant for polymers melts or solutions whereas slip of high solid dispersions is generally classified as apparent slip (Barnes 1999).

As a preventive technique (or, at least, to mitigate slippage effects), it is common to roughen the surface of the walls to disrupt the "depleted layer" (Barnes 1999; Fossen et al. 2013). Therefore, the suitable geometry choice is a fundamental part of the rheological analysis of materials prone to present apparent wall slip.

Despite the myriad of studies regarding the rheological behavior of waxy oils available in the literature and the research and development effort supported by oil companies, there are still open questions concerning the gelation process, yield stress appearance, apparent wall slip, and the role of wax chemical structures in the gel–fluid phase transition. Two of these issues are addressed here: (i) the pressure drop needed to restart the flow of a gelled waxy and (ii) the flow rate after gel breakage. The investigation comprises rheometric measurements of model waxy oils consisting of a macrocrystalline wax (3.0 and 7.5 wt%) added to a low-viscosity spindle mineral oil. Dynamic oscillatory and steady-state tests assessed the sample's rheological properties with different geometry configurations, including smooth and grooved concentric cylinders. The slippage effects were also considered in pressure drop and flow rate calculations through the balance between friction and pressure forces and modified Poiseuille equations.

Materials and methods

Sample preparation

Model oils were prepared under controlled conditions before each rheological test to avoid variation in thermal and shear histories. Linear macrocrystalline wax (29 carbons on average) with a melting temperature range of 56–58 °C was purchased from Sigma-Aldrich. Wax weight fractions of 3.0 wt% and 7.5 wt% were employed for 30 g fluid in each preparation. The wax content was based on waxy

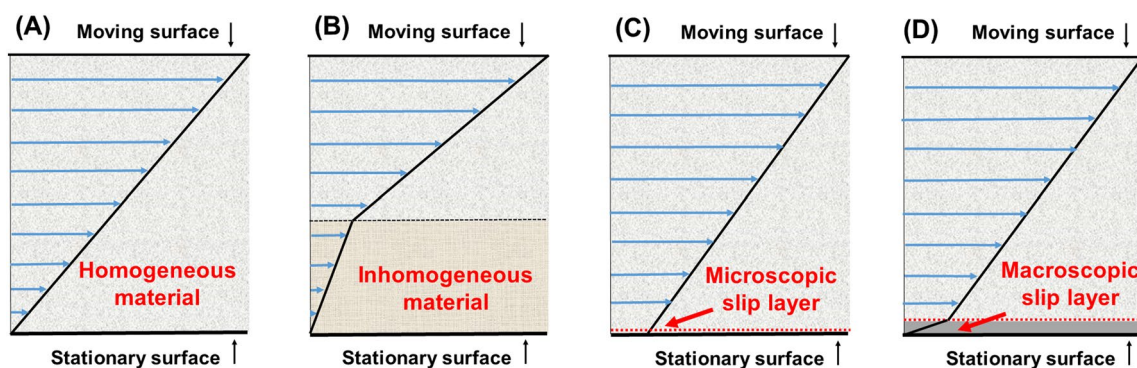


Fig. 1 The velocity profile for yield stress materials: **A** non-slip conditions, **B** shear banding phenomenon (material inhomogeneity is one possible cause), **C** true wall slip, and **D** apparent wall slip (adapted from Cloitre and Bonnecaze 2017)

crude oil compositions commonly encountered worldwide (Zougari and Sopkow 2007). A light mineral oil provided by Petrobras (315 °C boiling point, 852 kg/m³ density, and 2.39 × 10⁻³ Pa.s viscosity at 20 °C) was employed as a continuous phase. The mixture was placed in a beaker and heated to 85 °C for 15 min under magnetic stirring (C-MAQ HS7 from IKA) for complete wax solubilization. In this condition, the samples behave as a Newtonian liquid and can be loaded into the rheometer to be cooled in situ. The complete wax and mineral oil characterization can be found elsewhere (Marinho et al. 2021).

Rheological protocol

After preparation, samples were loaded on the DHR-3 stress-controlled rheometer (TA Instruments). Dynamic oscillatory tests were employed to assess the yield stress, and steady-state tests were performed to determine the flow curves of model oils at 4 °C. The rheological tests were conducted using concentric cylinder geometries with different surface roughness, as exhibited in Fig. 2.

Both rheological protocols were composed of 4 steps. The first three steps were identical:

- (i) 2 min of thermal equilibration at 50 °C;
- (ii) quiescent cooling from 50 to 4 °C at 1.0 °C/min;
- (iii) 30 min of isothermal holding at 4 °C to favor gelled structure development.

The last step for the dynamic oscillatory tests was an amplitude stress sweep at 4 °C and 1.0 Hz, from 1 to 500 Pa (3.0 wt% wax) or 1 Pa to 2700 Pa (7.5 wt% wax) in logarithmic mode. The yield stress was defined as the G' and G'' crossing point. In the case of steady-state tests, the last step was a shear rate controlled test using ascending logarithmic

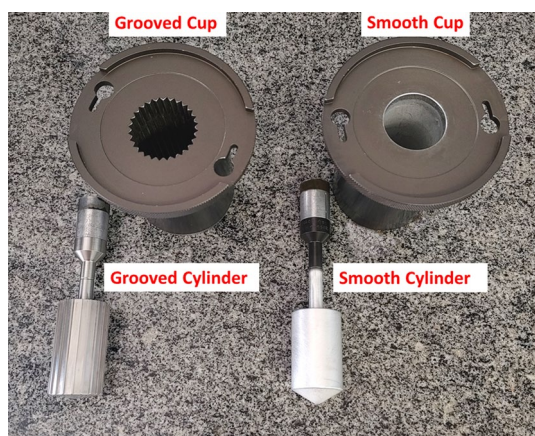


Fig. 2 Concentric cylinders and surface details. Slippage effects were observed when smooth surfaces were employed in rheometric tests

steps from 1.0 to 1000 s⁻¹, with an equilibration time of 150 s and 30 s sampling. The yield stress was estimated by extrapolating data to the zero shear rate. Another approach was a shear rate controlled test using descending logarithmic steps from 100 to 0.1 s⁻¹. Dynamic oscillatory tests were run in triplicate, whereas the steady-state tests were run in duplicate.

Theory

Consider a viscoplastic fluid in a steady, incompressible, and fully developed flow through a horizontal circular pipe. The balance between the pressure and friction forces can be represented by Eq. (1), where ΔP is the pressure drop, L is the pipe length filled with the fluid, σ_{rz} is the shear stress along the radius, and r is the radial coordinate in the cylindrical coordinate system ($r = 0$ in the center of the pipe) (Chhabra and Richardson 2008):

$$\Delta P \pi r^2 = \sigma_{rz} 2\pi r L \quad (1)$$

The left-hand side of Eq. 1 represents the pressure forces, and the right-hand side is the friction force developed during the flow. Isolating the pressure drop term ΔP in Eq. (1), we have Eq. (2):

$$\Delta P = 2\sigma_{rz} \frac{L}{r} \quad (2)$$

From Eq. (2), it is possible to estimate the pressure drop needed to restart pumping by the breakage of the waxy gelled structure, considering L as the clogged pipe portion and r as the total pipe radius (i.e., $r = R$). Eq. (2) applies to laminar and turbulent flow conditions because they are based on a simple force balance. No assumption has been made at this point concerning the type of flow or fluid behavior (García Blanco 2019).

The Power Law and Herschel–Bulkley (HB) rheological models, which describe a vast range of fluid behavior, are given in Eqs. (3) and (4), respectively:

$$\sigma_{rz} = k \left(\frac{du_z}{dr} \right)^n \quad (3)$$

$$\sigma_{rz} = \sigma_{HB} + m \left(\frac{du_z}{dr} \right)^n \quad (4)$$

In Eq. (3), k is the consistency index (Pa.sⁿ), u_z is the component of the fluid velocity in the z direction, and n is the flow behavior index (dimensionless). In Eq. (4), m is similar to parameter k , and σ_{HB} is the yield stress calculated from the HB model.

The oil flow rate (Q) after the gel breakage can be estimated from Eqs. (3) or (4), considering Power Law or

Herschel–Bulkley models, respectively. For example, when combining Eqs. (3) and (2) and integrating with respect to r , it is possible to obtain the velocity distribution for the fluid inside the pipe. The non-slip condition, which imposes that at the pipe walls, the velocity must be zero (for $r = R$, $u_z = 0$), allowing the integration constant determination. The flow rate is then calculated from $u_z(r)$ through Eq. 5, resulting in the flow rate for a Power Law fluid (Eq. 6):

$$Q = \int_0^R 2\pi r u_z dr \quad (5)$$

$$Q = \pi \left(\frac{n}{3n+1} \right) R^{(3+\frac{1}{n})} \left(\frac{\Delta P}{2kL} \right)^{\frac{1}{n}} \quad (6)$$

The same analytical development can be extended for the laminar flow of Herschel–Bulkley model fluids, resulting in Eq. (7), where φ is the ratio of the yield stress calculated from the Herschel–Bulkley model (σ_{HB}) and the stress on the pipe wall σ_w , calculated by Eq. (2) for $r = R$.

$$Q = n\pi R^3 \left(\frac{\sigma_w}{m} \right)^{\frac{1}{n}} (1-\varphi)^{\left(\frac{n+1}{n} \right)} \left[\frac{(1-\varphi)^2}{3n+1} + \frac{2\varphi(1-\varphi)}{2n+1} + \frac{\varphi^2}{n+1} \right] \quad (7)$$

Results and discussion

Dynamic oscillatory tests with geometries of different surface roughness were employed to assess the sample's yield stress. The prepared model oils could reproduce essential features of crude oil gels, exhibiting a low-temperature gel-like mechanical response to an imposed low-frequency oscillatory stress. Also, the gelled waxy oils presented a viscoelastic structure, exhibiting a linear viscoelastic region (LVR) and a yielding region during the amplitude stress sweep. The yielding region comprises the onset departure of the elastic modulus (G') from the LVR and the crossing point of G' and G'' . The yield stress is defined as the crossing point of G' and G'' (Fig. 3), which provides a reasonable and fast method to probe a wide experimental range (Tinsley and Prud'homme 2010).

As shown in Fig. 3, dynamic oscillatory tests with different geometries provided distinct yield stress values for the same sample under the same protocol. The results are summarized in Table 1 for model oils with 3.0 wt% wax and model oils with 7.5 wt% wax. It is worth mentioning that SC + SC indicates a smooth cylinder and a smooth cup, GC + SC indicates a grooved cylinder and a smooth cup, whereas GC + GC indicates a grooved cylinder and a grooved cup configuration. There is an astonishing decrease of ~80% in yield stress measurement for the complete smooth geometry (SC + SC) compared to the entire grooved

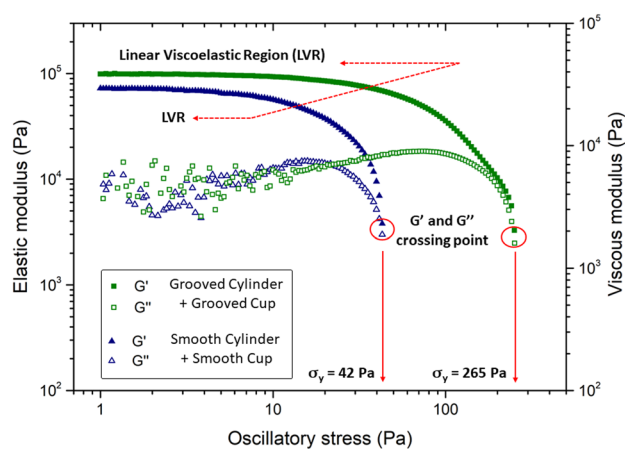


Fig. 3 Dynamic oscillatory test: a representative amplitude stress sweep at 4 °C and 1.0 Hz, from 1 to 500 Pa (3.0 wt% wax) in ascending logarithmic steps. Yield stress is defined as the oscillatory stress at G' and G'' crossing points

Table 1 Yield stress from dynamic oscillatory tests

Fluid	Geometry setup	σ_y (Pa)
3.0 wt% wax	Smooth Cylinder + Smooth Cup	40 ± 8
	Grooved Cylinder + Smooth Cup	64 ± 20
	Grooved Cylinder + Grooved Cup	259 ± 24
7.5 wt% wax	Smooth Cylinder + Smooth Cup	488 ± 100
	Grooved Cylinder + Smooth Cup	696 ± 130
	Grooved Cylinder + Grooved Cup	2,700 ± 252

geometry (GC + GC) regardless of the system composition, as already observed in Marinho et al. (2021) previous study. It is important to note that rheological results obtained from GC + GC geometry eliminate the slippage effects and represent the most conservative yield stress values. This geometry choice is more suitable to represent the internal walls of a flexible flowline, which presents many grooves in its extension. However, the internal wall of a coated brand-new rigid pipeline would be better represented with a smooth or partially smooth geometry. The recommendation on which geometry surface best represents a real application should be based on pipeline surface roughness provided or estimated beforehand (Marinho et al. 2021). Additionally, with continuous oil production, the pipeline's average roughness is expected to increase due to organic and inorganic deposition. In this sense, the limiting surface boundaries are covered as the authors provided measurements with smooth and grooved surfaces.

The yield stress of the gelled model oils was used to estimate the pressure drop required to restart a pipeline (ΔP_{REQ}) from Eq. (2), considering L as the clogged pipe portion. In Fig. 4, ΔP_{REQ} is presented as a function of the clogged pipe

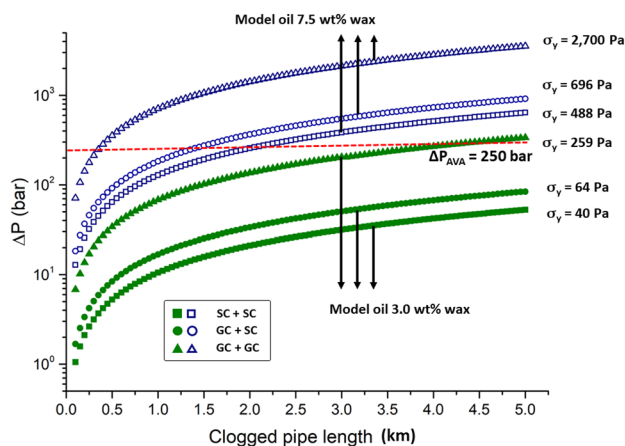


Fig. 4 Pressure drop estimation for restarting the flow for pipe with $D=6''$ and clogged portion ranging from 100 to 5000 m (model oil composed of 3.0 wt% and 7.5 wt% wax). The yield stress values (σ_y) were obtained at 4°C

length, varying from 100 to 5000 m, and a diameter $D=6''$ (a representative diameter in petroleum production). Model oils with 3.0 and 7.5 wt% wax were assessed. According to Lee et al. (2008), the restart of a pipeline blocked with gelled oil may result from the breakdown of the gel structure itself (cohesive failure), or it may occur because of the breakage at the pipe–gel interface (adhesive failure). The mechanism of cohesive yielding occurs when the applied stress exceeds the mechanical strength of the wax–oil gel structure. Thus, the process happens without wall slippage. Since it is very difficult to predict the failure mechanism in a real production scenario, the estimative of yield stress in terms of cohesive failure is extremely relevant because it is more conservative. For example, considering the maximum available pressure (ΔP_{AVA}) of 250 bar and model oil 3.0 wt% wax, the flow at a clogged pipeline with up to 3700 m could be restarted, considering the cohesive breakage of the gelled waxy structure (i.e., for measurements with GC + GC geometry, $\sigma_y = 259$ Pa). On the other hand, the flow could be restarted for the entire pipeline length (5000 m) for yield stress measurements made with smooth surfaces.

Considering the cohesive gel breakage, for systems with 7.5 wt% wax, the maximum length to restart a flow in a clogged pipeline is only 350 m. If the estimates were based on yield stress measurements employing only smooth surfaces (SC + SC), the maximum length would be 1950 m (5.6 times higher). These facts highlight the wax content's role and breakage mechanism on the flow restart. Thus, underestimated yield stress represents a significant drawback in estimating the restart pressure drop. It is important to mention that despite the representative wax composition, the prepared model oils do not account for the possible interaction effects of wax paraffin crystals with other common oil

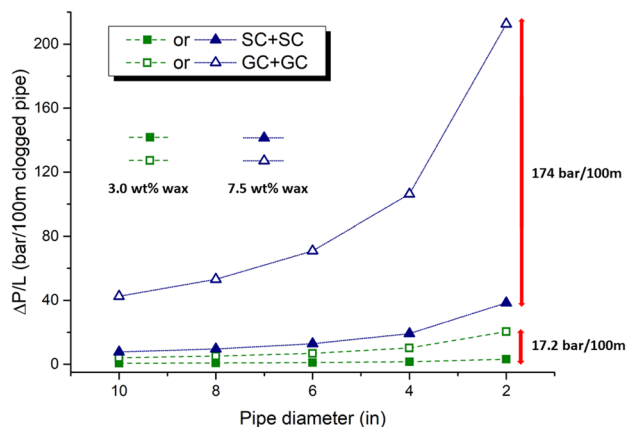


Fig. 5 Pressure drop for restart flow of clogged pipelines with $D=2, 4, 6, 8,$ and $10''$, model oil composition of 3.0 wt% (full symbols) and 7.5 wt% wax (open symbols), and different concentric cylinder surface roughness (note that x-axis is inverted)

components, such as resins, asphaltenes, water droplets, etc. Thus, assuming that previous results stand for all crude oils is not recommended. Although, as the interactions of waxy crystals drive the gelation process, waxy crude oils with a similar wax composition to the investigated model oils are expected to generate similar results when tested under similar conditions.

Figure 5 exhibits the ΔP_{REQ} for restarting 100 m of a clogged line as a function of pipe diameter. It is important to stress that pipes with diameters ranging from 4 to 10" are commonly encountered at offshore production operations (Chala et al. 2018). Considering the model oil with 3.0 wt% wax, for a pipe with 2" diameter ΔP_{REQ} varies from 3.15 bar/100 m (SC + SC) to 20.4 bar/100 m (GC + GC). For the 7.5 wt% wax in a 2" pipe, this difference is 174 bar/100 m. As one can observe, the pipe diameter has a considerable impact at ΔP_{REQ} for 7.5 wt% wax system. Also, ΔP_{REQ} progressively diverge as pipe diameter decreases and the wax content increases, representing a bottleneck for the correct pipeline design if surface roughness is not considered.

Model oils flow behavior was assessed through shear rate controlled tests using ascending logarithmic steps from 1.0 to 1000 s^{-1} experiments. Figure 6 exhibits the average shear stress and viscosity curves for the model oil 7.5 wt% wax. Equilibration time of 150 s and 30 s of sampling were employed at each shear rate. The slippage effect is evident when smooth surfaces (full symbols) are compared to grooved surfaces (open symbols). The presence of kinks (red circles) and the lower values of rheological properties, especially in the range of $1.0\text{--}100\text{ s}^{-1}$, significantly impact the flow rate calculations, as discussed next.

The parameters for Power Law and Herschel–Bulkley models were obtained based on the flow curves (Fig. 6) in

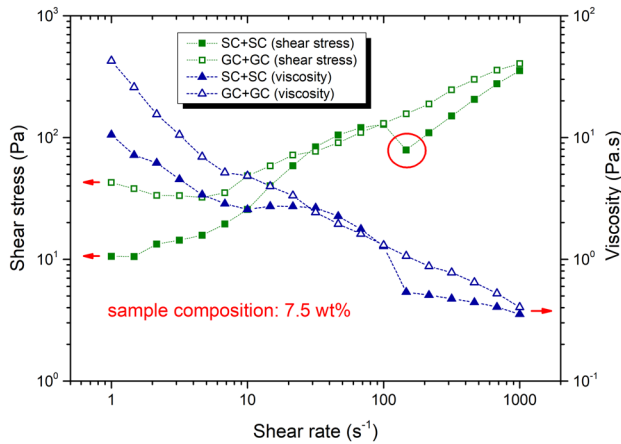


Fig. 6 Flow curves and viscosity curves for model waxy oil 7.5 wt% at 4 °C assessed with different cylinder surfaces

the range of 1.0–1000 s^{-1} and grouped in Table 2. The R^2 value evaluates the distance of the experimental data to the fitted regression line. As the parameter σ_{HB} (which corresponds to the yield stress obtained by the Herschel–Bulkley model) is dependent on the loading rate, differences may be expected when compared to the yield stress from dynamic oscillatory tests (Chang et al. 1998). However, the same trend can be observed: GC + GC geometries provided higher values for k and σ_{HB} for both model oils compositions. Also, slightly higher values of R^2 were obtained.

The calculated flow rate after gel breakage, according to the Power Law rheological model (Eq. 6), is presented in Fig. 7 as a function of clogged pipe length (1000–5000 m), considering 6" pipe diameter and $\Delta P_{AVA} = 250$ bar (these

are common figures in offshore petroleum production). As one can observe, the flow rates calculated for the model oil 3.0 wt% wax (both geometries) and model oil 7.5 wt% wax (SC + SC) are exceedingly higher than the reference productivity value of 1000 m^3/day (note that the reference flow rate production of 1000 m^3/day is not a limiting value, as offshore production wells can produce more than 10.000 m^3/day). The calculation for model oil 7.5 wt% wax (GC + GC) showed that the reference value is reached at about 3500 m of a clogged pipe. For both compositions, the flow rates presented a substantial decrease in the entire pipeline length assessed. When calculated with data from grooved geometries, the model oil 3.0 wt% wax demonstrated an average reduction of 8.13 times (standard deviation 0.81), and for 7.5 wt% an average decrease of 7.31 times (standard deviation 0.18) was observed. Since the same experimental protocol was applied to all tests, the slippage effect on rheometric measurements is the main responsible for these differences. Despite the considerable decrease in flow rates calculated with data from grooved geometries, the model oil 3.0 wt% wax presented unrealistic values for the entire pipeline length ranging from 1000 to 5000 m. This situation occurs because, after gel breakage, the pseudoplastic behavior of the waxy oil becomes very sharp (Fig. 6), and the Power Law model does not limit the viscosity to a minimum value. Thus, mathematically, the shear rate can go to infinity, and so the flow rate. Given the behavior of waxy oils after breakage, it is likely that the flow curves provide very low n parameters in most situations (e.g., 0.30–0.10) due to the pronounced pseudoplastic behavior. For comparison purposes, a polymer melt with parameters $k = 150 Pa \cdot s^{0.85}$ and $n = 0.85$

Table 2 Power Law and Herschel–Bulkley model parameters for model oils 3.0 and 7.5 wt% wax

Power Law model parameters		
Model oil 3.0 wt% wax	SC + SC ($R^2=0.93$)	GC + GC ($R^2=0.94$)
k [$Pa \cdot s^n$]	17.4	28.1
n [-]	0.298	0.321
Model oil 7.5 wt% wax	SC + SC ($R^2=0.95$)	GC + GC ($R^2=0.96$)
k [$Pa \cdot s^n$]	45.0	80.4
n [-]	0.272	0.305
Herschel–Bulkley model parameters		
Model oil 3.0 wt% wax	SC + SC ($R^2=0.94$)	GC + GC ($R^2=0.94$)
m [$Pa \cdot s^n$]	13.7	5.45
n [-]	0.436	0.674
σ_{HB} [Pa]	1.50	5.44
Model oil 7.5 wt% wax	SC + SC ($R^2=0.95$)	GC + GC ($R^2=0.97$)
m [$Pa \cdot s^n$]	14.6	14.0
n [-]	0.607	0.661
σ_{HB} [Pa]	15.3	45.4

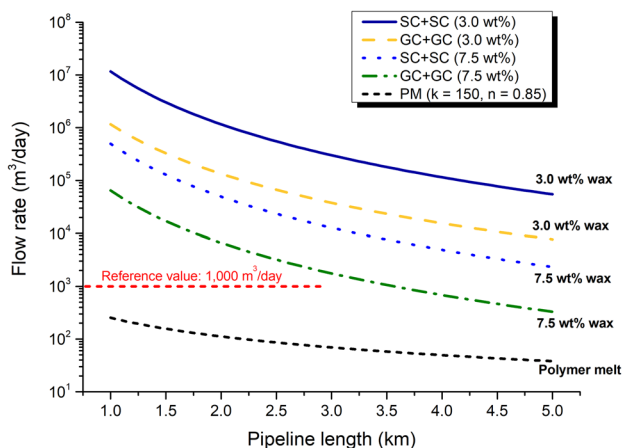


Fig. 7 Flow rate calculations based on the Power Law model parameters (Table 2) for the 3.0 wt% and 7.5 wt% waxy model oils and pipeline length ranging from 1000 to 5000 m, $D=6''$, $\Delta P_{AVA} = 250$ bar. A representative curve for a polymer melt ($k = 150 \text{ Pa}\cdot\text{s}^{0.85}$ and $n = 0.85$) was also added for comparison purposes

(Hristov et al. 2006) was added to Fig. 7, and feasible flow rate values were calculated. The extremely high viscosity during flow and the purely viscous fluid behavior ($n \sim 1$) contributed to this result.

Another approach to obtain Power Law or Herschel Bulkley model parameters and estimate the flow rate is to perform a shear rate controlled test in reverse mode (i.e., starting from a high shear rate and descending to lower values). Regarding industry applications, the direct mode experiment is more suitable to represent the restart pumping operation after a quiescent cooling for a long time (e.g., days). On the other hand, the reverse mode experiment better represents a quick shutting-down and restart operation (e.g., a few hours) where the oil was flowing subjected to high shear rates, and then the shear is continuously decreased due to well closure. In this case, a disrupted gelled structure better represents the material because the interactions leading to a strong gel could not ultimately form. Thus, direct and reverse flow curves can accommodate the limiting scenarios for extended and rapid pumping shutdown and restart operations, respectively. Also, in the reverse mode experiment, the high shear imposed on the samples can suppress the slippage effects because the fluid is completely unstructured, as in Fig. 8. In this case, the cylinder surfaces are almost equivalent at the flow measurement range of $100\text{--}1 \text{ s}^{-1}$. Although, due to the thixotropy behavior of the samples, there is a clear deviation of viscosity and stress for shear rates lower than 1.0 s^{-1} . The stress is higher for the grooved surfaces, and then higher viscosities are captured by this geometry.

The parameters for the Power Law model obtained by shear rate controlled experiments in the range of $100\text{--}0.1 \text{ s}^{-1}$ (i.e., reverse mode) were grouped in Table 3. The R^2 values

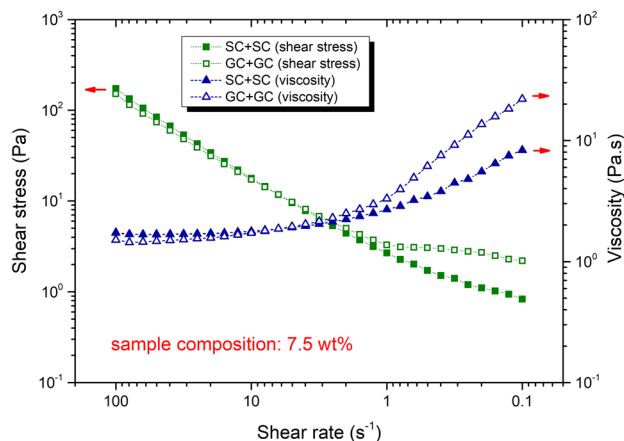


Fig. 8 Flow curves and viscosity curves in reverse mode for model waxy oil 7.5 wt% at 4°C assessed with different cylinder surfaces

indicated an excellent agreement between the experimental data and the fitted regression line.

Figure 9 exhibits the calculated flow rate in m^3/day (Eq. 6) as a function of the clogged pipeline length, considering the $6''$ pipe diameter and $\Delta P_{AVA} = 250$ bar. The square and triangle symbols represent the flow rates calculated from Table 3 data (reverse flow curves), whereas the dashed and dotted lines represent the flow rates calculated from Table 2 data (direct flow curves). The small values of parameter k and the parameter n close to the unity in Table 3 are reflected in flattened curves, yielding unrealistic flow rate values for all ranges assessed. Despite this fact, Fig. 9 provides valuable information: (i) surface roughness is still an important issue, as calculations based on grooved geometries provided lower flow rate values; (ii) starting the rheological test from 100 s^{-1} produced a highly sheared structure in a very short time, thus the pseudoplastic behavior is attenuated and n values are closer the unity (>0.94 for all cases), contributing to lower flow rate values in smaller pipe lengths, as $Q \sim 1/L$ and $Q \sim 1/n$; (iii) as apparent wall slip is more pronounced in low shear rates (Barnes 1995), the difference in flow rates for SC + SC and GC + GC is also lower (comparing the same oil wax content). This reflects that the fluid's structure was

Table 3 Power Law parameters for model oils 3.0 and 7.5 wt% wax obtained by flow curves in reverse mode

Power Law model parameters		
Model oil 3.0 wt% wax	SC + SC ($R^2=0.98$)	GC + GC ($R^2=0.97$)
k [$\text{Pa}\cdot\text{s}^n$]	0.315	0.422
n [–]	0.968	0.957
Model oil 7.5 wt% wax	SC + SC ($R^2=0.96$)	GC + GC ($R^2=0.98$)
k [$\text{Pa}\cdot\text{s}^n$]	1.72	3.22
n [–]	0.998	0.956

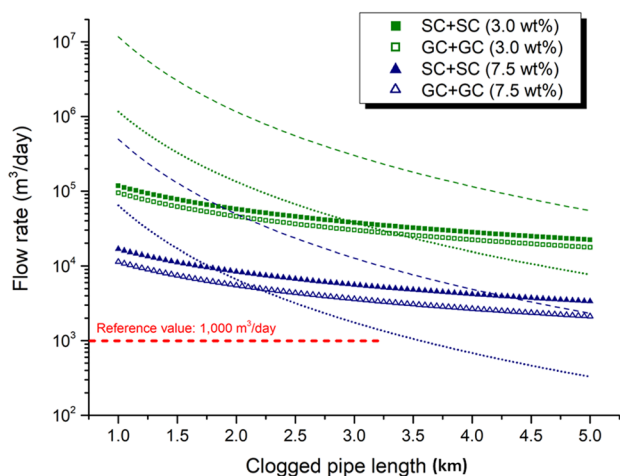


Fig. 9 Flow rate calculations based on the Power Law model parameters for the 3.0 wt% and 7.5 wt% waxy model oils and pipeline length ranging from 1000 to 5000 m, $D=6''$, $\Delta P_{AVA} = 250$ bar. Square and triangle symbols represent rheological data from shear rate controlled experiments from 100 to 0.1 s^{-1} . Dashed and dotted lines represent data taken from Fig. 7

already highly sheared when the experiment reached 1.0 s^{-1} . Consequently, the Power Law model parameters obtained from reverse mode flow curves are not recommended to estimate the flow rate involving waxy oils.

The Herschel–Bulkley parameters, obtained from shear rate controlled tests using ascending logarithmic steps from 1.0 to 1000 s^{-1} , were also employed to estimate the flow rates based on Eq. (7). Figure 10 exhibits the results for model oils 3.0 and 7.5 wt% wax, clogged pipes ranging from 1000 to 5000 m, pipe diameter 6" and $\Delta P_{AVA} = 250$ bar.

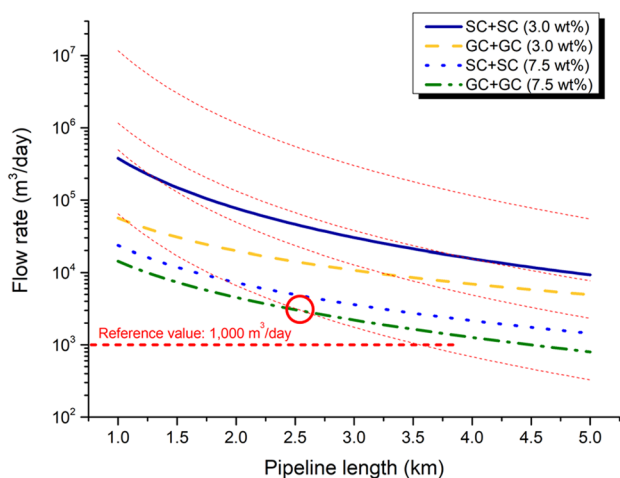


Fig. 10 Flow rate calculations based on the Herschel–Bulkley model for direct flow curves, waxy model oil 3.0 and 7.5 wt%, and pipeline length ranging from 1000 to 5000 m, $D=6''$, $\Delta P_{AVA} = 250$ bar. Red dotted lines represent data taken from Fig. 7

The results calculated from Power Law parameters are also shown as red dotted lines. As can be observed, the same experiments result in significant differences. For model oil 7.5 wt% tested with grooved geometry (GC + GC), there was a crossing point (red circle in Fig. 10) at ~ 2500 m. Before this length, the Herschel–Bulkley flow rate was lower than Power Law estimates. For all other cases, no crossing occurred, and Herschel–Bulkley flow rates were, on average, one order of magnitude lower than Power Law. The relatively higher n parameters for the HB model (Table 2) reflected in flattened curves, despite the presence σ_{HB} , unrealistic flow rate values (e.g. $Q > 10^4 \text{ m}^3/\text{day}$) were obtained. Also, due to apparent wall slip, the flow rate is exceedingly overestimated, although the difference becomes less pronounced when the wax content is increased.

Unlike the Power Law, the Herschel–Bulkley model has a third parameter σ_{HB} , which can be interpreted as fluid yield stress. In principle, this three-parameter model can fit the experimental data better and represent the flow of a yield stress fluid, such as a gelled waxy oil, more accurately. However, to precisely obtain σ_{HB} , the steady state must be achieved in rheometric experiments, especially at low shear rates (e.g., $0.001\text{--}1.0 \text{ s}^{-1}$). Regardless of the geometry surface employed, reaching a steady state at such a lower rate is a difficult task for complex fluids due to elasto-viscoplastic thixotropy behavior and the rheometer restrictions (torque and angular position sensors have limited sensibility). Therefore, it is likely that true σ_{HB} is higher than those calculated from the flow curves assessed in this study. In this regard, Fig. 11 exhibits flow rate estimates for progressively higher σ_{HB} for the model oil 7.5 wt% wax, with HB parameters $m = 14.0 \text{ Pa}\cdot\text{s}^{0.661}$, and $n = 0.661$ (Table 2), considering clogged pipe length ranging from 1000 to 5000 m, pipe diameter

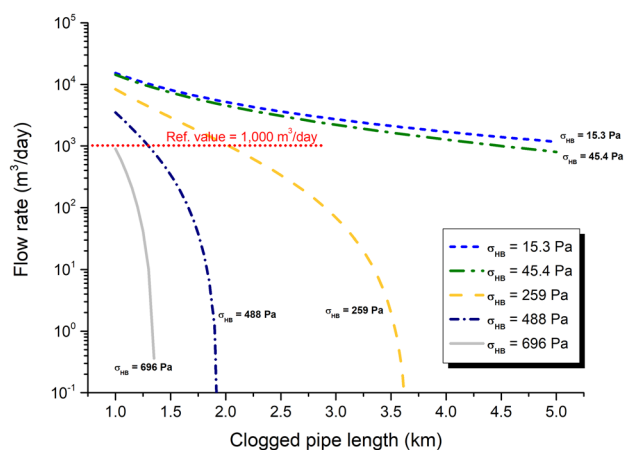


Fig. 11 Flow rate based on the Herschel–Bulkley model with several σ_{HB} values ($m = 14.0 \text{ Pa}\cdot\text{s}^{0.661}$, $n = 0.661$) for waxy oil 7.5 wt% and clogged pipeline varying from 1000 to 5000 m, $D=6''$, $\Delta P_{AVA} = 250$ bar

6" and $\Delta P_{AVA} = 250$ bar. The yield stress values of 259, 488, and 696 Pa were taken from dynamic oscillatory tests (Table 1), which were a more conservative estimation for this property. No flow rate was obtained for $\sigma_{HB} = 2700$ Pa because in such a situation, σ_{HB} overcomes the shear stress at the pipe wall. According to the results, the maximum clogged pipeline lengths for detectable flow rate ($Q > 0.1$ m³/day) are 3650 m, 1950 m, and 1350 m for σ_{HB} 259, 488, and 696 Pa. Thus, depending on the fluid yield stress, the Herschel–Bulkley model predicts no flow, which is physically observed in several practical situations.

Conclusions

In the case of waxy gel blockage occurrence in a real production scenario, two immediate questions demand an answer: (i) what is the pressure required to restart flow (ΔP_{REQ})? and (ii) what would be the flow rate in case of gelled structure breakage? This study addresses these two issues from the perspective of apparent wall slip effects in rheometric experiments. Model oils with 3.0 and 7.5 wt% wax were employed, and smooth and grooved geometries were tested. Two rheological models, Power Law and Herschel–Bulkley were compared in terms of flow rate estimates for a base scenario of maximum available pressure (ΔP_{AVA}) of 250 bar, pipe diameter of 6", and clogged pipe portion ranging from 1000 to 5000 m. Far from being random choices, these values reflect common figures in offshore petroleum production.

In terms of pressure drop, considering measurements with grooved geometries and assuming a maximum available pressure (ΔP_{AVA}) of 250 bar, the flow at a clogged pipeline with up to 370 m could be restarted for 7.5 wt% wax oil. If yield stress measurements were made with smooth geometries, a pipeline length of 1,950 m could be restarted. Also, it was verified that the ΔP_{REQ} calculations for different pipe diameters progressively diverge when smooth and grooved surfaces are used in rheometric tests. The situation worsens as the diameter decreases and wax content increases, representing a bottleneck for the correct pipeline design if surface roughness is not considered in the project.

The flow rate estimated with Power Law parameters exhibited exceedingly high values for 3.0 wt% model oil (e.g., $Q > 104$ m³/day), despite the different approaches used to obtain the flow curves (direct or reverse mode). Although surface roughness is still an important issue captured by the model, the Power Law displayed inferior performance compared to the Herschel–Bulkley model.

Herschel–Bulkley model had a better performance in terms of feasible flow rates due to the parameter σ_{HB} , which can be interpreted as fluid yield stress. Depending on the pipeline length and σ_{HB} value, the flow rate goes to zero, an

expected physical behavior not present in Power Law flow rate estimates. Further studies on the steady state conditions of the flow curves and numerical solutions for more complex rheological models (e.g., the Casson model) will be of great value for flow rate calculations of waxy oils in pipelines of varying lengths and diameters. An alternative to using more elaborate models would be to obtain the steady-state flow curve from very low shear rates (e.g., 0.001–1000 s⁻¹) in strain-controlled rheometers (SMT architecture, which has very low inertia) and use the parameters obtained by the Herschel–Bulkley model since Fig. 11 demonstrated much more realistic behavior when using more plausible values of the σ_{HB} parameter.

Acknowledgements The authors thank Petrobras/CENPES and CNPq (Conselho Nacional de Pesquisa e Desenvolvimento) for supporting this work.

Declarations

Conflict of interest The authors declare no competing interests relative to the publication of this study.

References

- Aiyejina A et al (2011) ‘Wax formation in oil pipelines: a critical review. *Int J Multiphase Flow* 37(7):671–694
- Barnes HA (1995) A review of slip (wall depletion) of polymer solutions, emulsions and particle suspensions in viscometers: its cause, character, and cure. *J Nonnewton Fluid Mech* 56:221–251
- Barnes HA (1999) The yield stress—a review or “panta roi”—everything flows? *J Nonnewton Fluid Mech* 81:133–178
- Cabanillas JP, Leiroz AT, Azevedo LFA (2016) Wax deposition in the presence of suspended crystals. *Energy Fuels* 30(1):1–11
- Chala GT, Sulaiman SA, Japper-jaafar A (2018) Flow start-up and transportation of waxy crude oil in pipelines—a review. *J Nonnewton Fluid Mech* 251:69–87
- Chang C, Boger DV, Nguyen QD (1998) The yielding of waxy crude oils. *Ind Eng Chem Res* 37(4):1551–1559
- Chhabra RP, Richardson JF (2008) *Non-newtonian flow and applied rheology*, 2nd edn. Elsevier, Berlin
- Cloitre M, Bonnecaze RT (2017) A review on wall slip in high solid dispersions. *Rheolog Acta Rheolog Acta* 56(3):283–385
- Davidson MR et al (2004) A model for restart of a pipeline with compressible gelled waxy crude oil. *J Nonnewton Fluid Mech* 123(2–3):269–280
- Fossen M, Oyangen T, Velle OJ (2013) Effect of the pipe diameter on the restart pressure of a gelled waxy crude Oil. *Energy Fuels* 27(7):3685–3691
- García Blanco YJ (2019) Visualization of viscoplastic fluid flow in an abrupt contraction using particle image velocimetry. Federal University of Technology, Paraná
- Hatzikiriakos SG (2015) Slip mechanisms in complex fluid flows. *Soft Matter R Soc Chem* 11(40):7851–7856
- Hristov V, Takács E, Vlachopoulos J (2006) Surface tearing and wall slip phenomena in extrusion of highly filled HDPE/wood flour composites. *Polym Eng Sci* 46:1205–1214
- Lee HS et al (2008) Waxy oil gel breaking mechanisms: adhesive versus cohesive failure. *Energy Fuels* 22(1):480–487

- Marinho TO et al (2021) Apparent wall slip effects on rheometric measurements of waxy gels. *J Rheol* 65(2):257–272
- Petter Rønningsen H (1992) Rheological behaviour of gelled, waxy North Sea crude oils. *J Pet Sci Eng* 7(3–4):177–213
- Saak AW, Jennings HM, Shah SP (2001) The influence of wall slip on yield stress and viscoelastic measurements of cement paste. *Cem Concr Res* 31(2):205–212
- Tinsley JF, Prud'homme RK (2010) Deposition apparatus to study the effects of polymers and asphaltenes upon wax deposition. *J Pet Sci Eng* 72(1–2):166–174
- Visintin RFG et al (2005) Rheological behavior and structural interpretation of waxy crude oil gels. *Langmuir* 21(14):6240–6249
- Walls HJ et al (2003) Yield stress and wall slip phenomena in colloidal silica gels. *J Rheol* 47(4):847–868
- Zougari MI, Sopkow T (2007) Introduction to crude oil wax crystallization kinetics: process modeling. *Ind Eng Chem Res* 46(4):1360–1368

Publisher's Note Springer Nature remains neutral with regard to jurisdictional claims in published maps and institutional affiliations.

Springer Nature or its licensor (e.g. a society or other partner) holds exclusive rights to this article under a publishing agreement with the author(s) or other rightsholder(s); author self-archiving of the accepted manuscript version of this article is solely governed by the terms of such publishing agreement and applicable law.